



**HAL**  
open science

## Polarimetric and photometric phase effects observed on transneptunian object (29981) 1999 TD10

P. Rousselot, Anny Chantal Levasseur-Regourd, K. Muinonen, J.-M. Petit

### ► To cite this version:

P. Rousselot, Anny Chantal Levasseur-Regourd, K. Muinonen, J.-M. Petit. Polarimetric and photometric phase effects observed on transneptunian object (29981) 1999 TD10. *Earth, Moon, and Planets*, 2005, 97 (3-4), pp.353-364. 10.1007/s11038-006-9079-5 . hal-00131437

**HAL Id: hal-00131437**

**<https://hal.science/hal-00131437>**

Submitted on 27 Oct 2021

**HAL** is a multi-disciplinary open access archive for the deposit and dissemination of scientific research documents, whether they are published or not. The documents may come from teaching and research institutions in France or abroad, or from public or private research centers.

L'archive ouverte pluridisciplinaire **HAL**, est destinée au dépôt et à la diffusion de documents scientifiques de niveau recherche, publiés ou non, émanant des établissements d'enseignement et de recherche français ou étrangers, des laboratoires publics ou privés.

POLARIMETRIC AND PHOTOMETRIC  
PHASE EFFECTS OBSERVED ON  
TRANSNEPTUNIAN OBJECT (29981)  
1999 TD<sub>10</sub>\*

P. ROUSSELOT<sup>1</sup>, A.C. LEVASSEUR-REGOURD<sup>2</sup>  
K. MUINONEN<sup>3</sup>, J.-M. PETIT<sup>1</sup>

<sup>1</sup>Observatoire de Besançon, BP 1615, 25010 Besançon Cedex, France

Email: roussetot@obs-besancon.fr

<sup>2</sup>Université Paris VI/ Aéronomie CNRS-IPSL, BP 3, 91371 Verrières, France

Email: aclr@aerov.jussieu.fr

<sup>3</sup>Observatory, PO Box 14, 00014 University of Helsinki, Finland

Email: muinonen@cc.helsinki.fi

Submitted to the special issue of *Earth, Moon and Planets*  
for Asteroids Comets Meteors 2005 meeting.

---

\*Based on observations obtained at the Cerro Paranal observatory of the European Southern Observatory (ESO) in Chile.

## Abstract

The Kuiper-Belt Object (29981) 1999 TD<sub>10</sub>, classified as a Scattered-Disk Object, has been observed at three different phase angles with the ESO 8.2-m VLT and FORS 1 instrument in polarimetric mode in November and December 2003. These observations have been used to compute the Stokes parameter  $q$ , which represents the linear polarization degree. We have also used the previously published photometric observations to improve the R-band phase function. The main conclusions are as follows: (i) a negative linear polarization degree decreasing with phase angle  $\alpha$  up to, at least,  $\alpha = 3^\circ$ , (ii)  $q \simeq -1.2\%$  for  $\alpha = 3^\circ$ , (iii) a possible color effect between the R and V band, the polarization degree being more negative in R.

The R-band polarimetric observations can be explained by the coherent-backscattering mechanism and fitted by a two-component Rayleigh-scatterer model for a spherical small body.

The rotation period of  $15.382 \pm 0.001$  hrs published by Mueller et al. (2004) and Choi et al. (2003) is confirmed. The R-band phase curve provides  $H = 8.35 \pm 0.02$  and  $G = -0.25 \pm 0.022$  parameters with the IAU H-G formalism.

**keywords:** transneptunian objects, polarimetry, photometry, (29981) 1999 TD<sub>10</sub>

# 1 Introduction

Kuiper Belt Objects (KBOs), whose existence was confirmed observationally in 1992 (Jewitt and Luu, 1993), represent an important clue to understand the formation and early evolution of the outer solar system. The relatively large number of known KBOs (1082 officially reported, when Centaurs are included, as of January 2006) provides more and more efficient tests for the different models of formation of the Kuiper Belt (e.g. Levison and Morbidelli, 2003).

The main problem encountered by astronomers to study the physical properties of KBOs comes from the faintness of these objects. Most of the observational work published so far was focused on color indices (see e.g. Doressoundiram et al., 2002; Hainaut and Delsanti, 2002). Quite a few results about rotational lightcurves (see e.g. Ortiz et al., 2003) and (noisy) visible and near-infrared spectra have also been published (see e.g. Brown, 2000a; Lazzarin et al., 2003; Fornasier et al., 2004).

This paper presents observational results based on a different approach to study the physical properties. Our observations are focused on the linear polarization degree of the solar light scattered by the target. It has been known for a long time that the solar light scattered by planetary surfaces presents a polarization, varying with the phase angle  $\alpha$  (angle Sun-target-observer) (Lyot 1929; Levasseur-Regourd, 2004). This effect has been studied for asteroids (see e.g. Belskaya et al., 2005) and cometary dust (see e.g. Levasseur-Regourd and Hadamcik, 2003) and constitutes a useful tool to improve our knowledge of the surface properties of KBOs.

This work presents also a reanalysis of previously published photometric

data. These data have been combined to improve the phase function curve of the target.

So far only two studies dedicated to polarimetric observations of KBOs / Centaurs have been published (Boehnhardt et al., 2004; Bagnulo et al., 2006). The observations published in these two papers have been obtained on Ixion and Quaoar and the Centaur Chiron. These three objects have revealed negative polarisation surges, with very different slopes, the steepest one being obtained for Ixion.

This paper presents observational data obtained on another KBO, (29981) 1999 TD<sub>10</sub>. It is a Scattered Disk Object (SDO) discovered on October 3, 1999 by Spacewatch. It is one of the brightest KBOs known and, due to its large eccentricity (see Table 1), currently one of the nearest KBOs to the Sun.

Different papers dedicated to observational studies of 1999 TD<sub>10</sub> have already been published, including three detailed studies, a first one focused on visible lightcurve and phase function curve (Rousselot et al., 2003), a second one to the rotation period and a claimed cometary activity (Choi et al., 2003) and a third one to the visible lightcurve and to near-infrared photometry (Mueller et al., 2004). Other papers and meeting presentations have also provided information on its color indices (Delsanti et al., 2001; Lederer et al., 2002), its lightcurve (Consolmagno et al., 2000; Ortiz and Gutiérrez, 2002) or its infrared spectrum (Brown 2000b).

Observational data are described in the next section. Section 3 presents our data analysis, both for the polarimetry and the photometry. The results are discussed in section 4.

## 2 Observations

The KBO (29981) 1999 TD<sub>10</sub> was observed with the 8.2 m Very Large Telescope (VLT) Unit Telescope 1 (called *Antu*), at the Cerro Paranal Observatory (Chile), managed by the European Southern Observatory (ESO). During the period November - December 2003, three different observing runs were conducted in service mode.

The observations were performed with a focal reducer and low dispersion spectrograph called *FOcal Reducer/low dispersion Spectrograph 1* (FORS 1). The detector is a thinned and coated Tektronix CCD chip of 2048×2048 pixels, with a pixel size of 24  $\mu\text{m}$  and a field of view 6.8×6.8 arcmin (0.2 arcsec/pixel, standard resolution). During our observations FORS 1 was functioning in imaging and polarimetric mode. This mode uses Wollaston prism as a beam splitting analyzer and one superachromatic  $\lambda/2$  phase retarder plate, allowing the measurement of the linear polarization.

The target was observed at four different position angles of the retarder plate (0, 22.5, 45, and 67.5°) through V and R broadband filters. The observing circumstances are presented in Table 2. The number of series is the amount of times where the above-mentioned observing cycles of the retarder plate are performed.

The data pre-processing has been performed with the MIDAS package. The BIAS has been computed by averaging about ten different raw bias images, after rejection of the minimum and maximum values for each pixel. The flat fields have been obtained by computing and normalizing the median of a set of twilight flat fields in imaging mode, without the retarder plate and the Wollaston prism. Different images of Highly Polarized Stan-

standard Stars were also obtained during the different observing runs. We used these images to compute the degree of linear polarisation of these stars and to check the results with the one provided by the ESO documentation (<http://www.eso.org/instruments/fors/inst/pola.html>).

## 3 Analysis

### 3.1 Polarimetry

Ordinary and extraordinary beams of the target were processed in a similar way following standard procedures of aperture photometry. The target fluxes were obtained with an aperture radius of 2.5 times the FWHM, and the sky background was determined using a 2 arcsec width annulus with internal radius of 5 arcsec.

For each series of exposures the following Stokes parameters were computed:

$$Q/I = 0.5 \left[ \left( \frac{f_o - f_e}{f_o + f_e} \right)_{\alpha'=0^\circ} - \left( \frac{f_o - f_e}{f_o + f_e} \right)_{\alpha'=45^\circ} \right]$$

$$U/I = 0.5 \left[ \left( \frac{f_o - f_e}{f_o + f_e} \right)_{\alpha'=22.5^\circ} - \left( \frac{f_o - f_e}{f_o + f_e} \right)_{\alpha'=67.5^\circ} \right]$$

where  $\alpha'$  is the position angle of the retarder plate, and  $f_o$  and  $f_e$  are, respectively, photon counts of the ordinary and extraordinary lightbeams.

Because these parameters correspond to the exposure frame, with a y-axis oriented along the South-North direction, it has been necessary to transform them to a reference frame related to the scattering plane on the target. This

plane is defined by the Sun-Target-Earth triangle. Calling  $\theta$  the angle between the direction 1999 TD<sub>10</sub>-North Pole and the direction Sun-1999 TD<sub>10</sub>, increased of 90° (in order to have a y-axis perpendicular to that plane), the transformation formulae can be written:

$$q = \cos(2\theta)(Q/I) + \sin(2\theta)(U/I)$$

$$u = -\sin(2\theta)(Q/I) + \cos(2\theta)(U/I)$$

Because of their definition  $q$  and  $u$  values can be either positive or negative.

The absolute polarization value  $p$  has also been computed. This parameter is always positive and is defined by :

$$p = \sqrt{(Q/I)^2 + (U/I)^2}$$

or by :

$$p = \sqrt{q^2 + u^2}$$

The  $q$ ,  $u$  and  $p$  parameters have been computed for each night by averaging the results obtained for different combinations of the retarder plates. These combinations correspond to a shift of one image between two successive series. For example if the images are labelled chronologically 1 2 3 4 5 6 7 and 8 (1 and 5 corresponding to  $\alpha' = 0^\circ$ , 2 and 6 to  $\alpha' = 22.5^\circ$ , 3 and 7 to  $\alpha' = 45^\circ$  and 4 and 8 to  $\alpha' = 67.5^\circ$ ), then the above mentioned parameters

are computed by using firstly the images *1 2 3 4*, secondly the images *2 3 4 5*, thirdly the images *3 4 5 6* etc... For the first observing night, two different sets of series have been used (with 12 different images the first series goes from *1 2 3 4* to *5 6 7 8* and the second one from *6 7 8 9* to *9 10 11 12*), providing two different measurements for the same night. The calculation of the standard deviations is based on the different data obtained for each series of combination of retarder plates.

This method provided good results for most of the data. A close examination of the resulting values lead, nevertheless, to the suppression of a few images that obviously produced wrong values when taken into account (for example the images obtained on November 29 with a highly polarized sky background).

To enhance the accuracy of the results for the last series of images (obtained during the last two nights), corresponding to very similar phase angle values, we have combined the polarimetric parameters obtained for the December 19<sup>th</sup> and 20<sup>th</sup> (the series of images used for these computations being not mixed with each other).

The results obtained are presented in Table 3. We have computed, for each parameter, the standard deviation values ( $\sigma$ ). Two different sets of results appear. The first one corresponds to a simple average of the different values obtained, when using the different possible combination of images (see above). The second one provides the results obtained with a  $\sigma$ -clipping algorithm. This algorithm rejects the values that deviate more than 1.5 times the standard deviation  $\sigma$  from the median. The remaining values are then averaged. In both cases the corresponding standard deviation is

given. Because the calculation of this standard deviation is based on data not completely independent of each other (because only one image out of four is changed at each time), the values given in the Table 3 are probably slightly underestimated. For most cases the results are identical, indicating a small dispersion in the results. Fig. 1 presents Stokes parameters  $q$  and  $u$ , respectively without and with the  $\sigma$ -clipping algorithm, as a function of the phase angle.

## 3.2 Photometry

As already mentioned 1999 TD<sub>10</sub> had been observed before this work, with photometric measurements published by Mueller et al. (2004) and Rousselot et al. (2003). It is possible to combine these data to improve the phase function of this target.

Mueller et al. present an accurate double-peaked lightcurve of 1999 TD<sub>10</sub> with a period of  $15.382 \pm 0.001$  hr (their Fig.7). This curve is based on R-band photometric data obtained by them and by Rousselot et al. (2003). With these results it is also possible to derive a new phase curve, more accurate than the one published by Rousselot et al.

We applied the method described by Rousselot et al. (2003, 2005) to the combined data set of Mueller et al. and Rousselot et al. (2003) to compute a more accurate phase function curve. The first step consists in recomputing the lightcurve in order to check the results published by Mueller et al.). The main difference between our method and that of these authors is that we solve explicitly for the phase effect at the same time as for the lightcurve, while Mueller et al. used an assumed phase function to first

correct their magnitude estimates for the phase effect, and then solved for the lightcurve (they did not compute, consequently, the phase function). The best period is  $15\text{hr}22\text{mn}57\text{s}\pm 3\text{s}$ , or  $15.3825\pm 0.001$  hr, in perfect agreement with the values published by Mueller et al. and Choi et al. (2003). The corresponding lightcurve is given in Fig. 2.

Using these period and lightcurve, we have derived the phase curve presented in Fig. 3. We fitted this curve using both the H-G formalism and the linear fit as used by, e.g, Schaefer & Rabinowitz (2002) and Sheppard & Jewitt (2002). The H-G formalism gives a very good fit for  $H=8.35\pm 0.02$  and  $G=-0.25\pm 0.022$  (curved dashed line in upper part of Fig. 3). The linear fit (dash-dotted straight line on the same figure) is definitely less satisfactory. The best fit corresponds to:  $m_0 = 8.45$  and  $\beta = 0.12$  (linear dash-dotted line in upper part of Fig. 3). It should be pointed out that the negative G value provided by this calculation is indicative of the difficulties of the H-G system to describe KBO opposition effect (see Rousselot et al. 2005 for a more detailed discussion on this topic).

## 4 Discussion

We explain the polarimetric and photometric phase curves of 1999 TD<sub>10</sub> through extensive numerical simulations of coherent backscattering by Rayleigh scatterers (Muinonen 2004; Muinonen et al. 2002b). Based on the V-band albedo obtained with Spitzer observations (Stansberry et al., 2005) and the (V-R) color of 1999 TD<sub>10</sub> (Rousselot et al. 2003), we used for the simulations geometric R-band albedos in the 0.06–0.12 range.

The observations have been tentatively interpreted through existing coherent backscattering computations for altogether 360 spherical media of Rayleigh scatterers. The computations entailed 18 different single-scattering albedos  $\tilde{\omega} = 0.05, 0.10, \dots, 0.90$  and 20 different dimensionless mean free paths  $k\ell = 2\pi\ell/\lambda = 10, 20, 30, \dots, 100, 120, 140, \dots, 200, 250, 300, \dots, 400, 500$  ( $k$  and  $\lambda$  are the wave number and wavelength).

For a fixed geometric albedo, the one-component Rayleigh-scattering model parameterized by the single pair of single-scattering albedo and mean free path results in polarizations that are larger than the observed polarizations. For 1999 TD<sub>10</sub>, we confirmed the poorness of the fits by comparing the polarimetric observations against all 360 one-component media of Rayleigh scatterers.

As in Boehnhardt et al.(2004) for Ixion, we then examined a two-component Rayleigh-scattering model consisting of dark and bright scatterers. There are five parameters in such a model: two single-scattering albedos and two mean free paths, and the weight factor  $w_d$  for the dark component (the weight factor of the bright component being  $w_b = 1 - w_d$ ). Fixing the geometric albedo fixes the weight factor, reducing the number of free parameters to four. After a systematic study of physically realistic combinations of the two kinds of scatterers, satisfactory fits were obtained for the polarization across the entire range of possible geometric albedos of  $p_R \in [0.06, 0.12]$ .

Among the solutions for 1999 TD<sub>10</sub>, there are ones that, qualitatively, resemble those obtained for Ixion by Boehnhardt et al. (2004), eventhough the polarimetric phase curves differ substantially. We can fit the 1999 TD<sub>10</sub> observations by a two-component model where the dark component shows a

mean free path substantially longer than the wavelength and where the bright component shows a short mean free path. Example model parameters with the corresponding rms value of the fit are given in Table 4 with the actual fits depicted in Fig. 4. Note that the fits are by no means unambiguous. They rather demonstrate the capability of the two-component model to explain the observations.

Besides the polarization fits, approximate brightness fits (lower part of Fig. 3) were obtained by varying the absolute magnitude  $H_R$ , residual enhancement factor  $\zeta_R$ , angular peak width  $d_R$ , and slope parameter  $k_R$  for a linear-exponential phase dependence multiplying the coherent backscattering contribution (Muinonen et al. 2002a). In the present context, the enhancement factor thus represents a residual enhancement due to, e.g., mutual shadowing among regolith structures large compared to the wavelength.

## 5 Conclusion

This work presents the first polarimetric observations of 1999 TD<sub>10</sub>. These observations have revealed: (i) a negative linear polarization degree which decreases with the phase angle  $\alpha$  up to, at least,  $\alpha = 3^\circ$ , (ii)  $q \simeq -1.2\%$  for  $\alpha = 3^\circ$ , (iii) a possible color effect between the R and V band, the polarization degree being more negative in R.

The R-band polarimetric observations can be explained by the coherent-backscattering mechanism and fitted by a two-component Rayleigh-scatterer model for a spherical small body. For a realistic example geometric albedo of  $p_R = 0.085$ , 95% of the small-body surface area would be covered by a

medium of single-scattering albedo  $\tilde{\omega} = 0.30$  and dimensionless mean free path  $k\ell = 250$  whereas, for the remaining 5% of the surface, the numbers would be 0.90 and 10.

We also present a re-analysis of the already published photometric data of 1999 TD<sub>10</sub>, permitting an improvement of the R-band phase function. The rotation period of  $15.382 \pm 0.001$  hrs published by Mueller et al. (2004) and Choi et al. (2003) is confirmed. The R-band phase curve provides  $H=8.35 \pm 0.11$  and  $G=-0.25 \pm 0.022$  parameters with the IAU H-G formalism.

The polarimetric results are only a first step for this object, since more observational data and more thorough coherent-backscattering modeling for 1999 TD<sub>10</sub> would be necessary to put more constraints on its surface properties. Such a work is beyond the scope of the present study.

## References

- Bagnulo, S., Boehnhardt, H., Muinonen, K., Kolokolova, L., Belskaya, I., Barucci, M.A.: 2006, *Astron. Astrophys.*, in press
- Belskaya, I. N., Shkuratov, Yu. G., Efimov, Yu. S., Shakhovskoy, N. M., Gil-Hutton, R., Cellino, A., Zubko, E. S., Ovcharenko, A. A., Bondarenko, S. Yu., Shevchenko, V. G., Fornasier, S., and Barbieri, C.: 2005, *Icarus* **178**, 213-221
- Boehnhardt, H., Bagnulo, S., Muinonen, K., Barucci, M.A., Kolokolova, L., Dotto, E., and Tozzi, G.P.: 2004, *Astron. Astrophys.* **415**, L21-L25
- Brown, M.E.: 2000a, *Astron. J.* **119**, 977-983
- Brown, M.E.: 2000b, American Astronomical Society, DPS meeting #32, #20.08

- Choi, Y. J., Brosch, N., Prialnik, D.: 2003, *Icarus* **165**, 101-111
- Consolmagno, G.J., Tegler, S.C., Rettig, T., and Romanishin, W.: 2000, *Bulletin of the American Astronomical Society* **32**, 1032
- Delsanti, A.C., Boehnhardt, H., Barrera, L., Meech, K. J., Sekiguchi, T., and Hainaut, O. R.: 2001, *Astron. Astrophys.* **380**, 347-358
- Doressoundiram, A., Peixinho, N., de Bergh, C., Fornasier, S., Thébault, P., Barucci, M. A., and Veillet, C.: 2002, *Astron. J.* **124**, 2279-2296
- Fornasier, S., Dotto, E., Barucci, M.A., and Barbieri, C.: 2004, *Astron. Astrophys.* **422**, L43-L46
- Hainaut, O.R., and Delsanti, A.C.: 2002, *Astron. Astrophys.* **389**, 641-664
- Jewitt, D., Luu, J.: 1993, *Nature* **362**, 730-732
- Lazzarin, M., Barucci, M.A., Boehnhardt, H., Tozzi, G. P., de Bergh, C., and Dotto, E.: 2003, *Astron. J.* **125**, 1554-1558
- Lederer, S.M., Jarvis K.S., and Vilas, F. 2002: Asteroids, Comets, Meteor meeting, Berlin, 29 July - 2 August 2002
- Levasseur-Regourd, A.C. 2004: 'Polarimetry of dust in the solar system: remote observations, in-situ measurements and experimental simulations', In Photopolarimetry in remote sensing, G. Videen, Y. Yatskiv and M. Mishchenko eds. NATO Science Series, Kluwer, 393-410
- Levasseur-Regourd, A.C., and Hadamcik, E.: 2003, *JQSRT*, 79, 903-910
- Levison, H.F., and Morbidelli, A.: 2003, *Nature* **426**, 419-421
- Lyot, B., 1929, 'Recherche sur la polarisation de la lumière des planètes et de quelques substances terrestres', Ann. Obs. Paris, PhD

Mueller, B.E.A, Hergenrother, C.W., Samarasinha, N.H., Campins, H., and McCarthy Jr, D.W.: 2004, *Icarus* **171**, 506-515

Muinsonen, K.: 2004, *Waves in Random Media* **14**(3), 365-388

Muinsonen, K., Piironen, J., Kaasalainen, S. and Cellino, A.:2002a, *Memorie Della Società Astronomica Italiana—Journal of the Italian Astronomical Society* **73**, 716-721

Muinsonen, K., Piironen, J., Shkuratov, Yu. G., Ovcharenko, A., and Clark, B. E.: 2002b, 'Asteroid photometric and polarimetric phase effects' In *Asteroids III* (W. Bottke, R. P. Binzel, A. Cellino, P. Paolicchi, Eds., University of Arizona Press, Tucson, Arizona, U.S.A.), 123-138

Ortiz, J.L., and Gutiérrez, P.J.: 2002, Asteroids, Comets, Meteor meeting, Berlin, 29 July - 2 August 2002

Ortiz, J.L., Gutiérrez, P.J., Casanova, V., and Sota, A.: 2003, *Astron. Astrophys.* **407**, 1149-1155

Rousselot, P., Petit, J.M., Poulet, F., Lacerda, P., and Ortiz, J.: 2003, *Astron. Astrophys.* **407**, 1139-1147

Rousselot, P., Petit, J.M., Poulet, F., and Sergeev, A.: 2005, *Icarus* **176**, 478-491

Schaefer, B.E., and Rabinowitz, D.L.: 2002, *Icarus* **160**, 52-58

Sheppard, S.S., and Jewitt, D.C.: 2002, *Astron. Journal* **124**, 1757-1775

Stansberry, J. A., Cruikshank, D. P., Grundy, W. G., Margot, J. L., Emery, J. P., Fernandez, Y. R., and Rieke, G. H.:2005, American Astronomical Society, DPS meeting #37, #52.05

Table 1: Orbital characteristics of 1999 TD<sub>10</sub>.

| a (AU) | e    | q (AU) | Q (AU) | i    |
|--------|------|--------|--------|------|
| 95.1   | 0.87 | 12.28  | 178.0  | 6.0° |

Table 2: Observing circumstances for 1999 TD<sub>10</sub> (R: Heliocentric distance (AU);  $\Delta$ : Geocentric distance (AU);  $\alpha$ : phase angle). For the sky CLR means clear and PHO mean photometric sky.

| UT Date      | Start/end (UT) | $\Delta$ | R     | $\alpha$ | Filter(exp. time) | Number of series | Sky |
|--------------|----------------|----------|-------|----------|-------------------|------------------|-----|
| 2003 Nov. 12 | 00:08/01:28    | 13.01    | 13.98 | 0.77°    | R(305s)           | 3                | CLR |
| 2003 Nov. 29 | 00:52/02:28    | 13.15    | 14.02 | 1.93°    | R(225s)/V(335s)   | 2                | CLR |
| 2003 Nov. 30 | 04:54/06:29    | 13.16    | 14.02 | 2.00°    | R(225s)/V(335s)   | 2                | PHO |
| 2003 Dec. 19 | 00:54/03:32    | 13.40    | 14.06 | 3.05°    | R(225s)/V(335s)   | 3                | CLR |
| 2003 Dec. 20 | 03:38/05:07    | 13.42    | 14.06 | 3.10°    | R(500s)/V(700s)   | 1                | CLR |

Table 3: Polarimetric parameters computed with the observational data.  $N$  is the number of series of images used to compute the average value given in the Table. The origin of the rotational phase has arbitrarily been chosen as equal to zero for the first observation. It is based on the rotation period published by Mueller et al. (2004).

| Filter | Phase angle  | $q/\sigma_q$ (%) | $u/\sigma_u$ (%) | $p/\sigma_p$ (%) | $N$ | Rotational Phase    |
|--------|--------------|------------------|------------------|------------------|-----|---------------------|
| R      | $0.77^\circ$ | $-0.75 \pm 0.14$ | $0.38 \pm 0.09$  | $0.85 \pm 0.13$  | 5   | 0.00-0.05           |
|        |              | $-0.71 \pm 0.13$ | $0.38 \pm 0.09$  | $0.81 \pm 0.12$  |     |                     |
| R      | $0.77^\circ$ | $-0.64 \pm 0.07$ | $0.06 \pm 0.16$  | $0.66 \pm 0.07$  | 4   | 0.04-0.09           |
|        |              | $-0.64 \pm 0.07$ | $0.06 \pm 0.16$  | $0.66 \pm 0.07$  |     |                     |
| R      | $2.00^\circ$ | $-0.85 \pm 0.26$ | $-0.04 \pm 0.25$ | $0.87 \pm 0.26$  | 5   | 0.39-0.50           |
|        |              | $-0.85 \pm 0.26$ | $-0.04 \pm 0.25$ | $0.87 \pm 0.26$  |     |                     |
| V      | $2.00^\circ$ | $-0.68 \pm 0.21$ | $-0.13 \pm 0.11$ | $0.71 \pm 0.17$  |     | 0.39-0.50           |
|        |              | $-0.78 \pm 0.07$ | $-0.13 \pm 0.11$ | $0.71 \pm 0.17$  |     |                     |
| R      | $3.07^\circ$ | $-1.20 \pm 0.26$ | $0.31 \pm 0.33$  | $1.28 \pm 0.25$  | 9   | 0.51-0.61+0.77-0.95 |
|        |              | $-1.36 \pm 0.21$ | $0.24 \pm 0.27$  | $1.35 \pm 0.17$  |     |                     |
| V      | $3.07^\circ$ | $-0.93 \pm 0.19$ | $0.19 \pm 0.39$  | $1.02 \pm 0.18$  | 9   | 0.51-0.61+0.77-0.95 |
|        |              | $-0.88 \pm 0.15$ | $0.27 \pm 0.34$  | $1.01 \pm 0.12$  |     |                     |

Table 4: The best-fit coherent-backscattering model parameters for 1999 TD<sub>10</sub> for the geometric albedo  $p_R = 0.085$ . We give the single-scattering albedos  $\tilde{\omega}$  and dimensionless mean free paths  $k\ell$  for the dark (subscript  $d$ ) and bright components ( $b$ ), the weight of the dark component  $w_d$ , the rms values of the polarimetric fit, as well as the R-band absolute magnitude  $H_R$ , residual enhancement factor  $\zeta_R$ , angular peak width  $d_R$ , and slope parameter  $k_R$  for a residual linear-exponential model.

| Object                | $\tilde{\omega}_d$ | $\ell_d$ | $\tilde{\omega}_b$ | $\ell_b$ | $w_d$ | rms    | $H_R$ | $\zeta_R$ | $d_R$       | $k_R$          |
|-----------------------|--------------------|----------|--------------------|----------|-------|--------|-------|-----------|-------------|----------------|
| 1999 TD <sub>10</sub> | 0.30               | 250      | 0.90               | 10       | 0.95  | 0.058% | 8.39  | 1.5       | $2.0^\circ$ | $0.005/^\circ$ |

### Figure captions:

**Figure 1:** Linear polarization degree  $q$  represented as a function of the phase angle  $\alpha$ . A: Data obtained without  $\sigma$ -clipping algorithm. B: Data obtained when the  $\sigma$ -clipping algorithm is used.

**Figure 2:** Lightcurve plot of the combined data set of Mueller et al. (2004) (solid triangles) and Rousselot et al. (2003) (solid circles) in R-band, using a best fit period of 15.3825 hr. The magnitudes have been corrected for a heliocentric and geocentric distance of 1 AU and for the phase effect shown in Fig. 3, using phase angle  $0.35^\circ$  as a reference. The dashed line represents the best fit for these data using the previous period.

**Figure 3:** Phase function curve derived from the data published by Rousselot et al. 2003 (crosses) and Mueller et al. 2004 (circles). Upper Fig.: the dashed line shows the best fit function in the H-G formalism, while the dash-dotted line represents the best linear fit to the data. Lower Fig.: the dashed line shows the best fit function model of coherent backscattering and shadowing.

**Figure 4:** The R-band polarization as explained by a model of coherent backscattering and shadowing. The values used are the ones with the sigma-clipping algorithm. See the text for more details.

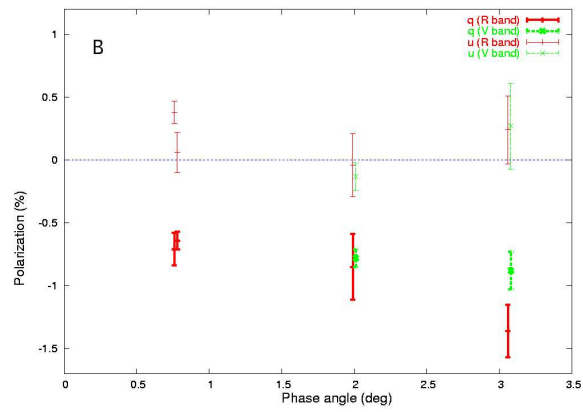
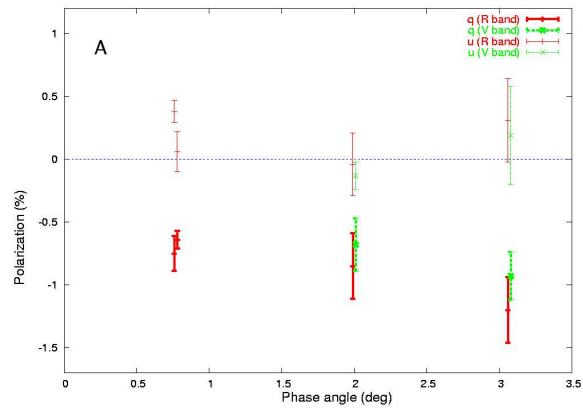


Figure 1:

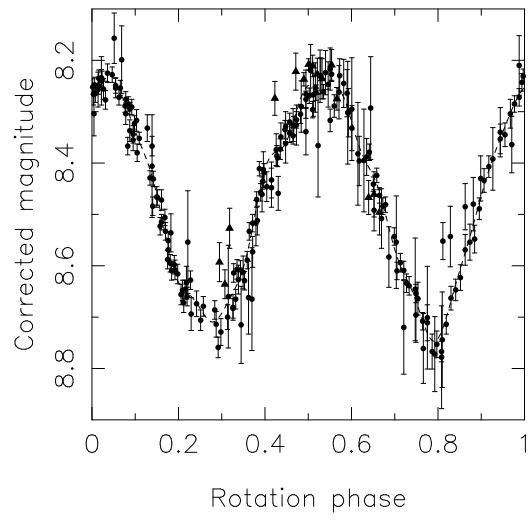


Figure 2:

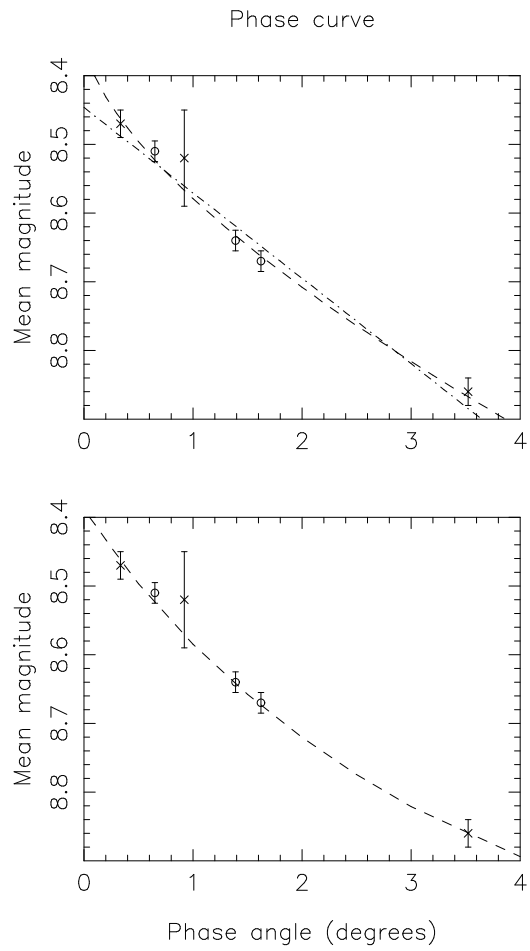


Figure 3:

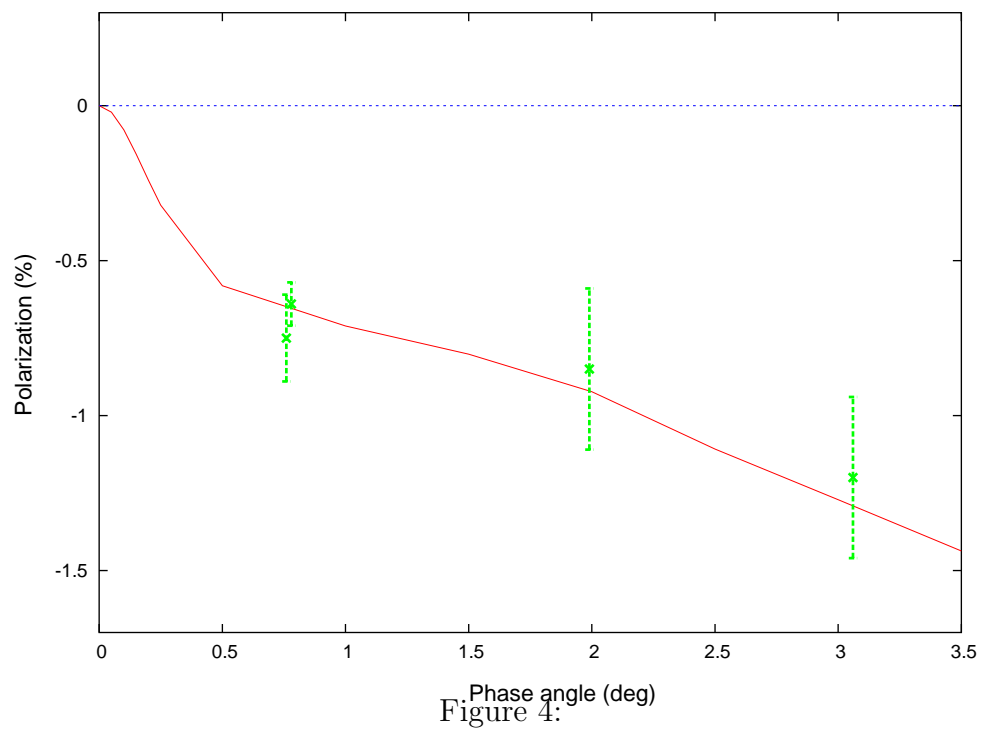


Figure 4: